2-P

March 1973
Technical Report—Part A

AUTOMATED THEMATIC MAPPING AND CHANGE DETECTION OF ERTS-1 IMAGES

Diffraction pattern analysis of
ERTS-1 images

Nicholas Gramenopoulos, Francis J. Corbett
Optical Systems Division
Itek Corporation
10 Maguire Road
Lexington, Massachusetts 02173

Prepared for
GODDARD SPACE FLIGHT CENTER
Greenbelt, Maryland 20771

TECHNICAL REPORT STANDARD TITLE PAGE

1. Report No.	2. Government Accession No.	3. Recipient's Catalog No.

4. Title and Subtitle	5. Report Date
Automated Thematic Mapping and Change Detection of ERTS-1 Images	March 1973
	6. Performing Organization Code: Itek 73-8217-2
7. Author(s): N. Gramenopoulos, F. J. Corbett	8. Performing Organization Report No.: PFR 73-033
9. Performing Organization Name and Address: Optical Systems Division, Itek Corporation, 10 Maguire Road, Lexington, Massachusetts 02173	10. Work Unit No.
	11. Contract or Grant No.: NAS5-21766
12. Sponsoring Agency Name and Address: Goddard Space Flight Center, Greenbelt, Maryland 20771, Technical Monitor: Edmund F. Szajna	13. Type of Report and Period Covered: Technical Report Part - A
	14. Sponsoring Agency Code

15. Supplementary Notes

16. Abstract

Automatic and accurate image processing techniques are essential to full utilization of ERTS-1 photography. In pursuit of this, terrain types in the ERTS-1 photography will be classified by spatial signatures. Diffraction patterns from selected ERTS-1 images have been developed optically and are being analyzed to identify unique signatures for various terrain types. Spatial signatures have been definitely identified for cultivated land and certain urban areas.

A Fourier plane mask has been developed that greatly facilitates the analysis of the diffraction patterns.

17. Key Words (Selected by Author(s))	18. Distribution Statement
Interpretation techniques development, coherent optical information extraction techniques, terrain spatial signatures	

19. Security Classif. (of this report)	20. Security Classif. (of this page)	21. No. of Pages	22. Price
Unclassified	Unclassified		

SUMMARY

Category 8:	Interpretation Techniques Development
Subcategory C:	Classification and Pattern Recognition
Title:	Automated Thematic Mapping and Change Detection of ERTS-1 Images
Subtitle:	Diffraction Pattern Analysis of ERTS-1 Images
Authors:	N. Gramenopoulos, F. Corbett

ABSTRACT

Automatic and accurate image processing techniques are essential to full utilization of ERTS-1 photography. In pursuit of this, terrain types in the ERTS-1 photography will be classified by spatial signatures. Diffraction patterns from selected ERTS-1 images have been developed optically and are being analyzed to identify unique signatures for various terrain types.

Spatial signatures have been definitely identified for cultivated land and certain urban areas.

A Fourier plane mask has been developed that greatly facilitates the analysis of the diffraction patterns.

SUMMARY

Category 8:	Interpretation Techniques Development
Subcategory H:	Coherent Optical Information Extraction Techniques
Title:	Automated Thematic Mapping and Change Detection of ERTS-1 Images
Subtitle:	Diffraction Pattern Analysis of ERTS-1 Images
Authors:	N. Gramenopoulos, F. Corbett

ABSTRACT

Automatic and accurate image processing techniques are essential to full utilization of ERTS-1 photography. In pursuit of this, terrain types in the ERTS-1 photography will be classified by spatial signatures. Diffraction patterns from selected ERTS-1 images have been developed optically and are being analyzed to identify unique signatures for various terrain types.

Spatial signatures have been definitely identified for cultivated land and certain urban areas.

A Fourier plane mask has been developed that greatly facilitates the analysis of the diffraction patterns.

CONTENTS

FIGURES

TABLE

1. INTRODUCTION

Multispectral digital recognition techniques ignore the spatial information in an image. Yet, the information conveyed to a human observer by a black and white image is purely spatial. The automated classification of resources can be significantly improved and expanded by utilizing the spatial information in the images. Terrain types can be digitally recognized if they can be associated with spatial signatures that can be defined as unique patterns in a set of measurements, involving a small area of an image. The area size is bounded on the low end by the image resolution and on the high end by image characteristics. In other words, the average area analyzed should be significantly larger than image resolution (at least 10 × 10 pixels) and should not be so large as to include more than one type of terrain.

The measurements that may be made and the technique for extracting a spatial signature are not restricted. The Fourier transform of an image is a convenient means for isolating and extracting spatial signatures. The reason is that repetitive image characteristics are transformed into discrete frequencies that can be more easily isolated.

The spatial signatures that can be isolated are dependent on image characteristics such as resolution and scale. For the ERTS images, spatial signatures are determined by examining the Fourier transforms from both ERTS and aircraft images for the same geographical area. The aircraft images, being of higher resolution, are useful for identifying spatial signatures that are very weak in the Fourier transforms of the ERTS images. The most efficient way to establish terrain signatures for the ERTS images is optically, using the Fourier transforming properties of lenses.

The purpose of this report is to describe the technical progress of the diffraction-pattern analysis task.

Section 2 describes the experimental procedure for photographing the diffraction patterns and the development of masks used as Fourier plane filters to enhance the spatial signatures.

Section 3 describes a number of diffraction patterns from ERTS-1 images and aircraft photography and the results of their preliminary analysis. Spatial signatures have been isolated for cultivated land and certain urban areas. Additional analysis is required to isolate signatures for mountainous terrain and deserts.

Section 4 describes the conclusions drawn from the diffraction-pattern analysis.

Section 5 describes the diffraction-pattern analysis to be conducted early in 1973 and the utilization of the spatial signatures developed.

Section 6 lists the significant results achieved during this reporting period.

2. EXPERIMENTAL PROCEDURE

In the ERTS-1 images, the terrain types that one would like to recognize consist of:

- Mountains
- Desert or range
- Cultivated land
- Clouds
- Urban areas
- Hills
- Rivers
- Bodies of water
- Transportation networks

Fourier transforms of images displaying one terrain type provide a means for isolating terrain signatures. However, for some terrain types, the Fourier transforms may not be the optimum transformation for isolating the signatures.

The Fraunhofer diffraction pattern of an image is related to its Fourier transform. It is well known that, if a transparency is introduced into the front focal plane of a lens and illuminated by a coherent plane parallel beam, the lens will form an image at its back focal plane whose amplitude distribution is the Fourier transform of the amplitude transmission of the transparency. Specifically,†

$$U_f(x_f,y_f) = \frac{A}{j\lambda f} \iint_{-\infty}^{+\infty} t_a(x_o,y_o) \exp\left[-j\frac{2\pi}{\lambda f}(x_o x_f + y_o y_f)\right] dx_o dy_o \qquad (2\text{-}1)$$

where $U_f(x_f,y_f)$ is the amplitude distribution at the back focal plane, x_f,y_f are the coordinates at the back focal plane, λ is the wavelength of light, f is the focal length of the lens, A is the amplitude of the illuminating beam, and $t_a(x_o,y_o)$ is the amplitude transmission of the transparency. The diffraction pattern $D(x_f,y_f)$ is the amplitude squared of $U_f(x_f,y_f)$:

$$D(x_f,y_f) = U_f(x_f,y_f) \cdot U^*(x_f,y_f) = |U(x_f,y_f)|^2 \qquad (2\text{-}2)$$

In addition

$$t_a(x_o,y_o) = [T(x_o,y_o)]^{1/2} e^{+j\Phi(x_o,y_o)} \qquad (2\text{-}3)$$

where $T(x_o,y_o)$ is the intensity transmission of the transparency for coherent light and $\Phi(x_o,y_o)$ is a phase function due to emulsion thickness that is unrelated to the image.

It is obvious from the above equations that the diffraction pattern is not equal to the Fourier transform of the image. However, the diffraction pattern is useful because it has the same general structure as the Fourier transform.

---

† J. W. Goodman, Introduction to Fourier Optics, McGraw-Hill Book Co., Inc., New York (1968), p. 86.

Noise or errors in the diffraction pattern associated with the phase function $\Phi(x_o,y_o)$ can be eliminated by inserting the transparency in a liquid gate filled with a refractive index matching fluid.

The optical bench employed is shown in Figure 2-1. The laser has a wavelength of 632.8 nanometers and its beam is expanded and filtered to produce a beam that is gaussian in intensity. The primary lens forming the diffraction pattern has a focal length of 48 inches, to produce large diffraction patterns. The frequency scale of the diffraction pattern is proportional to the focal length of the lens and the wavelength of illumination.

To reduce the overall dimensions of the bench, the transparency is located near the lens rather than on its front focal plane. The result is that a quadratic phase factor now multiplies $U_f(x_f,y_f)$ but does not affect the diffraction patterns.

Liquid gates are not employed because they are inconvenient when diffraction patterns from a large number of images are to be obtained. The optical bench permits photographing of the diffraction patterns and the images simultaneously. It also allows photometric measurements of any part (rings or wedges) of the diffraction patterns.

The ERTS images selected are described in Section 3.2. The images initially employed were positive transparencies on $9\frac{1}{2}$-inch-wide film. They produced small diffraction patterns. It was decided, therefore, to reduce the scale of the ERTS-1 images by a factor of three and develop the reduced images to a gamma of two to compensate for the square root factor in Equation 2-1. The maximum resolution in the reduced transparencies was estimated at about 25 line pairs per millimeter.

The diffraction patterns have some artifacts not related to the terrain images:

- Rings due to the circular aperture employed to limit the image area being transformed; these rings are also present in a digitally computed Fourier transform
- Two frequency spots due to the line structure present in the ERTS images; the line structure is a characteristic of the multispectral scanner and electron beam recorder system
- Artifacts due to the optical bench, such as lens aberrations, laser beam nonuniformity, phase modulation by the transparencies
- The central order is so bright that it usually saturates the film over a sizable area surrounding the central order and masks low frequency components.

To eliminate or suppress artifacts in the diffraction patterns, a mask is employed when photographing the diffraction patterns. The mask is itself the photograph of the diffraction pattern of an image area (from ERTS images) with no detail, such as areas of water from lakes or the ocean.

Figure 2-2 provides a comparison of a typical diffraction pattern with and without the mask. It is obvious that the mask enhances the low frequency structure of the diffraction pattern and suppresses artifacts. For this reason, these masks have been used consistently.

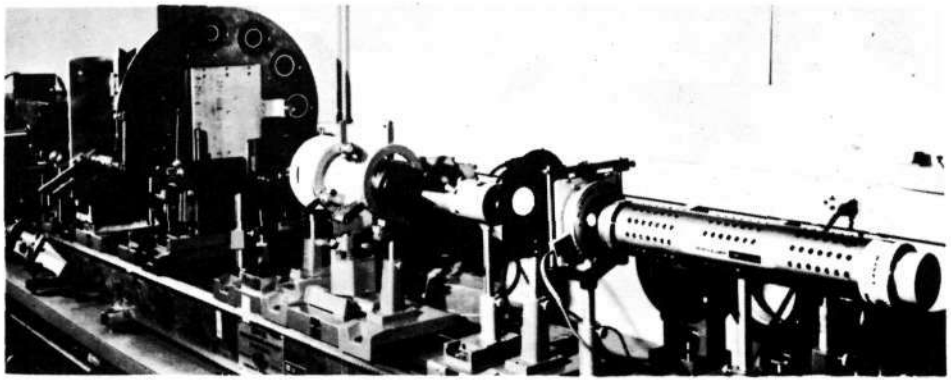

Power spectrum optical bench

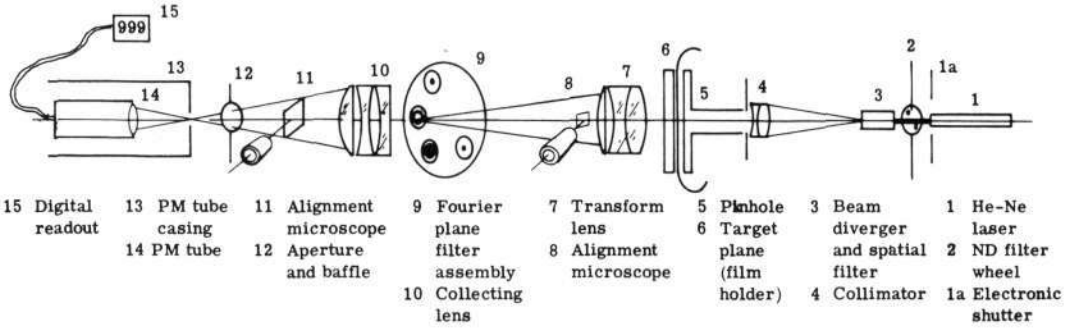

Diagram of power spectrum apparatus

Figure 2-1 — Coherent optical bench

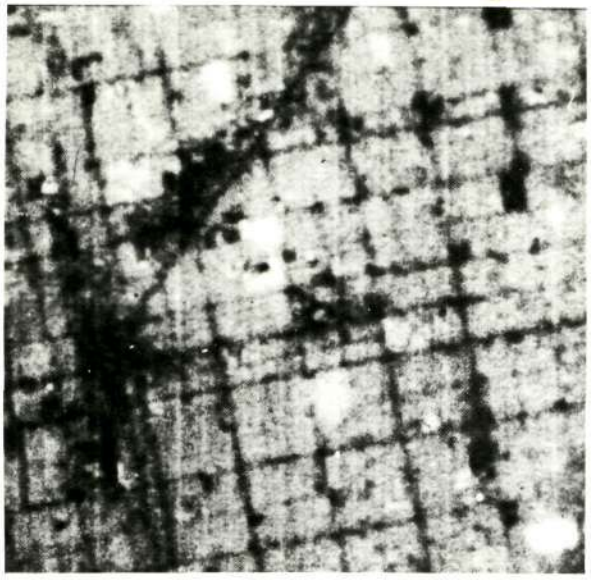

Phoenix, Arizona. ERTS-217-1

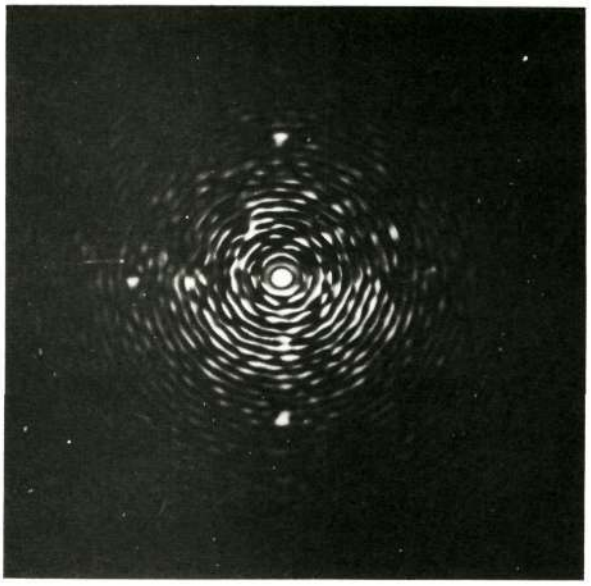

Diffraction pattern with mask. 217-1

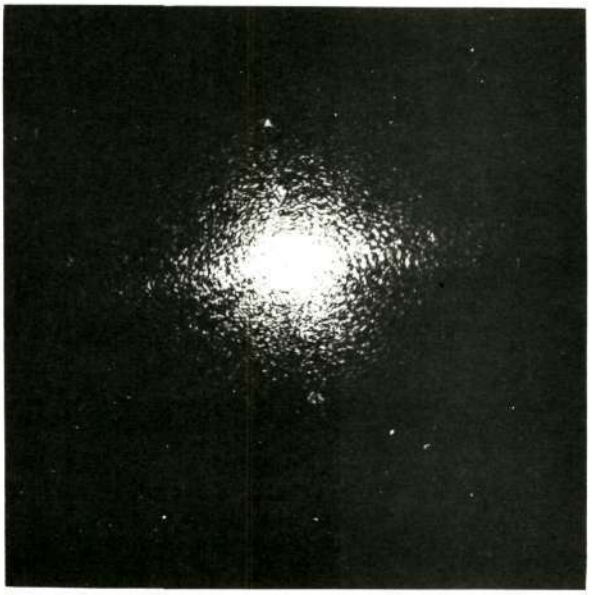

Diffraction pattern without mask. 217-1

Figure 2-2— Phoenix, Arizona. Two diffraction patterns from same area: one with a spatial filter, one without

3. ANALYSIS OF DIFFRACTION PATTERNS

3.1 COMPARISON OF DIFFRACTION PATTERNS: ERTS-1 IMAGES VERSUS AIRCRAFT PHOTOGRAPHY

A part of the initial program was concerned with a comparison of features in ERTS and aircraft photography. The purpose was to attempt to show similiarities in the diffraction patterns from the two types of imagery. The aircraft images, being of larger scale, are useful for identifying spatial signatures that are very weak in the Fourier transforms of the ERTS images. In particular, it was hoped to develop spatial signatures for urban areas in the ERTS-1 images by comparing diffraction patterns from ERTS-1 images and aircraft photography for the same urban areas. Diffraction patterns were produced for New Orleans and several small communities at the Gulf Coast near Brownsville, Texas. Diffraction patterns were photographed with and without the Fourier plane mask discussed in Section 2.

Figure 3-1 shows a high altitude aircraft photograph of New Orleans from mission 201 and diffraction patterns from three areas of New Orleans. Figure 3-2 shows ERTS-1 image No. 1070-16037-5 with New Orleans in the lower center area and the diffraction pattern of the encircled area. Only the major arteries in New Orleans are visible in the ERTS-1 image.

In the diffraction patterns of the aircraft photograph, intersecting lines are associated with the parallel street patterns. Each set of parallel streets produces a line in the diffraction pattern oriented perpendicular to the street direction. In the ERTS-1 image, only the major arteries diffract light in directions normal to the arteries. For that reason, the high frequency content of the diffraction pattern from the ERTS-1 image is rather weak. Nevertheless, a definite structure is evident in the diffraction pattern of Figure 3-2. There are a few preferred directions along which more light has been diffracted. These can be associated with specific major highways of New Orleans. The structure in the diffraction pattern of Figure 3-2 can be correctly considered to be a signature for intersecting major highways. It becomes a signature for an urban area only if highway intersections occur within urban areas. While intersections of two highways can occur in a nonurban area, intersections of three or more highways indicate, with a high probability, an urban area. Figure 3-3 shows a high altitude aircraft photograph of the Texas coast north of Brownsville, Texas. There are four communities from east to west: Palm Beach, Port Isabel, Bayside, and Laguna Vista. Figure 3-4 shows the diffraction patterns from two communities of Figure 3-3. Figure 3-5 shows an enlargement of the Texas coast from the ERTS-1 image No. 1038-16314. Diffraction patterns from the encircled areas corresponding with the encircled towns in Figure 3-3 are shown in Figure 3-6. These were obtained by using the Fourier plane mask, described in Section 2, to eliminate artifacts. The four communities are not detected visually in the ERTS-1 image. Such detection involves recognizing the street pattern against the recorder line pattern in the ERTS-1 image. If the street pattern existed in the ERTS-1 image, it may become evident as frequency components in the diffraction patterns.

The diffraction patterns of Figure 3-4 show frequency spots that correspond to the spacing of the parallel streets in the communities of Figure 3-3. The diffraction patterns of Figure 3-6

show no frequency spots that can be related to the street patterns of the small communities.

3.2 ERTS-1 TERRAIN SIGNATURES

3.2.1 Description of ERTS-1 Diffraction Patterns

Table 3-1 lists the ERTS-1 images that were employed for developing spatial signatures for various types of terrain. The New Orleans image (1070-16073-5) has been discussed in Section 3.1 as Figure 3-2. The remaining images are shown in Figures 3-7, 3-10, 3-12, 3-14, 3-16, and 3-18. Diffraction patterns were obtained from the image areas identified by numbered circles. The corresponding diffraction patterns are shown in Figures 3-8, 3-9, 3-11, 3-13, 3-15, 3-17, and 3-19 respectively. The diffraction patterns were photographed by using the Fourier plane mask discussed in Section 2.

Table 3-1—List of ERTS-1 Images

Image Identification	Area Covered
030 NASA ERTS E-1070-17495-5	Imperial Valley, California
084 NASA ERTS E-1070-16073-5	New Orleans Area
098 NASA ERTS E-1041-18253-5	Cascade Mountains, Washington
101 NASA ERTS E-1015-17415-7	Salt Lake City Area
116 NASA ERTS E-1040-18201-5	Cascade Mountain Area
181 NASA ERTS E-1031-17325-5	Phoenix Area
217 NASA ERTS E-1-31-17325-7	Phoenix Area

Rings in the diffraction patterns are associated with the aperture only, not with image detail within the aperture. The spacing (d) between adjacent dark bands in the Airy disk is $d = 1.22\lambda f/a$, where λ is the wavelength of light, f is the focal length of the lens, and a is the aperture diameter.

Increasing the aperture decreases the ring spacing and improves the resolution of the diffraction pattern. However, the central order becomes very intense and obscures low frequency components even though a Fourier plane mask is being employed. In addition, if the aperture is too large, the image will include more than one type of terrain.

The aperture size was adjusted so that low frequencies are not obscured by the central order while the ring structure is not so coarse that frequency spots due to the image are lost by excessive broadening. A sinusoidal frequency ν present in the image will produce a spot located at a distance γ from the center of the diffraction pattern such that $\gamma = f\lambda\nu$, where f is the focal length of the lens and λ is the wavelength of light. The aperture was set at 2 millimeters and it produced ring spacing of 0.471 millimeter, which corresponds to a frequency of 0.61 cycle per millimeter in the image.

The important spectral content of the diffraction patterns exists for frequencies larger than 1 cycle per millimeter. This frequency corresponds to about 1/3 cycle per millimeter for the original image size ($9^1/_2$-inch format) or 1 cycle per 3 kilometers on the ground.

3.2.2 Cultivated Land Signatures

In Figure 3-8, diffraction pattern No. 030-3 from a portion of the Imperial Valley displays a unique signature for the cultivated land of this region. The signature consists of two orthogonal rows of frequency spots. One of the rows is slightly tilted to the horizontal. A third row, which is horizontal, is barely visible and is a result of the line structure of the image. The two orthogonal rows are due to the square fields, whose size and dimensions are highly repeatable. The frequency spots are multiples of the fundamental frequency.

That so many high frequency spots are visible is due to the Fourier plane mask, In Figure 3-9, there are two diffraction patterns, Nos. 084-1 and 084-3, from cultivated land along the Mississippi River. The fields are elongated rectangles, with their long dimension approximately normal to the river. In diffraction pattern No. 084-3, there are two orthogonal rows of spots but the spacing of the spots in the two rows is different because of the elongated rectangular shape of the farms. In diffraction pattern No. 084-1, there is only one row of spots. Orthogonal to it, there is an almost continuous linear structure instead of another row of spots. In Figure 3-2(a) the farms appear to have the same shape as the farms that produced diffraction pattern No. 084-3. However, crops in adjacent farms appear to be similar (in terms of reflectance) and the result is that the farms appear to be wider and of irregular shape. This comparison brings out a crucial point: the diffraction pattern is affected not only by the field size and shape but also by the crop reflectances.

In Figure 3-14, there are two encircled areas that contain circular fields. In Figure 3-15, diffraction pattern No. 116-1 has a structure that corresponds to the farm pattern. There is a broken circular ring that resulted from the interference at the circular aperture with the numerous circular fields. Then, there are at least two frequency spots at about double the frequency of the circular ring. These appear to belong to two orthogonal and equally spaced rows of frequency spots, which are due to the uniform spacing of circular fields in rows and columns.

Diffraction pattern No. 116-2 displays a complex pattern. There appears to be a near vertical row of frequency spots and a much fainter horizontal row normal to the vertical one. Also, there are two orthogonal fans (light diffracted into broad lines) and a smaller fan located about 45 degrees to the other two farms. The orthogonal rows appear to be related to the regular spacing of the circular farms. Displacement of frequency spots in the row is slightly smaller than the displacement of the frequency spots for diffraction pattern No. 116-1. This agrees with the observation that the farms for diffraction pattern No. 116-2 appear larger than the farms for diffraction pattern No. 116-1. The origin of the fans is not obvious, but they may be related to the variation of reflectance in the farms (white, gray, and black).

There are two cultivated areas in Figure 3-16, with diffraction patterns No. 181-2 and 181-3 shown in Figure 3-17. Both patterns have two orthogonal rows of frequency spots, which are, however, very weak. In addition, there is a lot of light diffracted in other directions. The farms in Figure 3-16 are characterized by many vertical and horizontal edges. However, due to the reflectance of the crops, the edges appear to be random in size and distribution. In turn, the diffraction patterns are characterized by many frequency spots. However, the principal spots marked in the figure do correspond to the predominant farm size in that region, which is a quarter-mile-square section.

In conclusion, it appears that cultivated land can be identified by a signature, in the diffraction patterns, that consists of two orthogonal rows of frequency spots. The spacing of the frequency spots may not be the same in both rows. For some images, the signature must be detected in a diffraction pattern that contains many other strong frequency components.

3.2.3 Mountainous Terrain Signatures

In Figure 3-8, diffraction pattern No. 030-1 shows diffraction of light (fans) in a direction normal to the mountain ridges (see Figure 3-7). The fans are rather broad and contain strong frequency components.

In Figure 3-11, there are three diffraction patterns from mountainous terrain in the Cascade Mountains. These diffraction patterns have characteristics similar to diffraction pattern No. 030-1.

Diffraction pattern No. 101-3 in Figure 3-13 was produced by the mountainous terrain of Figure 3-12. This pattern is also characterized by a broad fan in a direction normal to the mountain ridges. In Figure 3-15, diffraction patterns Nos. 116-3 and 116-4 are from the mountainous terrain of Figure 3-14. Diffraction pattern No. 116-4 is again similar to the other patterns of mountainous terrain. Pattern No. 116-3 displays an extremely broadened fan, which can be attributed to variations in the orientation of the corresponding mountain ridges in Figure 3-14.

In Figure 3-17, diffraction pattern No. 181-1 was produced by mountainous terrain from Figure 3-16. This pattern also shows a broad fan normal to the mountain ridges. In conclusion, the diffraction patterns of mountainous terrain show diffraction of light along broad fans normal to mountain ridges. An obvious, unique signature for mountains has not been identified yet.

3.2.4 Urban Area Signatures

In Figure 3-8, diffraction pattern No. 030-2 was produced by a small town in the Imperial Valley (see Figure 3-7). There is nothing distinctive about this pattern, and diffraction of light along fans appears to be due to the edges of the cultivated region surrounding the town.

In Figure 3-13, diffraction patterns No. 101-1 and 101-2 are from the urban area of Salt Lake City. Several major arteries are seen in the encircled areas in Figure 3-12. The diffraction patterns show several rows of frequency spots. The horizontal row is due to the line structure of the image (a scanner/recorder artifact). Tilted to that row is a pair of orthogonal rows due to the repetitive pattern of orthogonal major arteries of Salt Lake City.

In Figure 3-17, diffraction pattern No. 181-4 is produced by an area of Phoenix from the image of Figure 3-16. This pattern shows only one horizontal row of frequency spots owing to the line structure of the image.

In Figure 3-19, diffraction pattern No. 217-1 shows two orthogonal rows of frequency spots owing to the major street pattern of Phoenix (see Figure 3-18). In conclusion, urban areas can be identified by signatures resulting from patterns of parallel major arteries. This signature becomes evident only in the IR-2 (0.8- to 1.1-micrometer) band for the cities of Phoenix and Salt Lake. This difference in signature from the same area photographed in two different spectral bands is seen by comparing the relative strengths of the diffracted spots in Figures 3-17 (No. 181-4) and 3-19 (No. 217-1). In New Orleans, such a street pattern does not exist. Instead, New Orleans is characterized by intersections of major highways that are visible in the red band image. It appears that a signature for small towns does not exist since secondary street patterns are not resolved.

3.2.5 Other Terrain Signatures

Diffraction patterns were obtained also from other terrain features such as broken clouds, rivers, and transportation networks. These have not been presented because they are not expected to produce signatures.

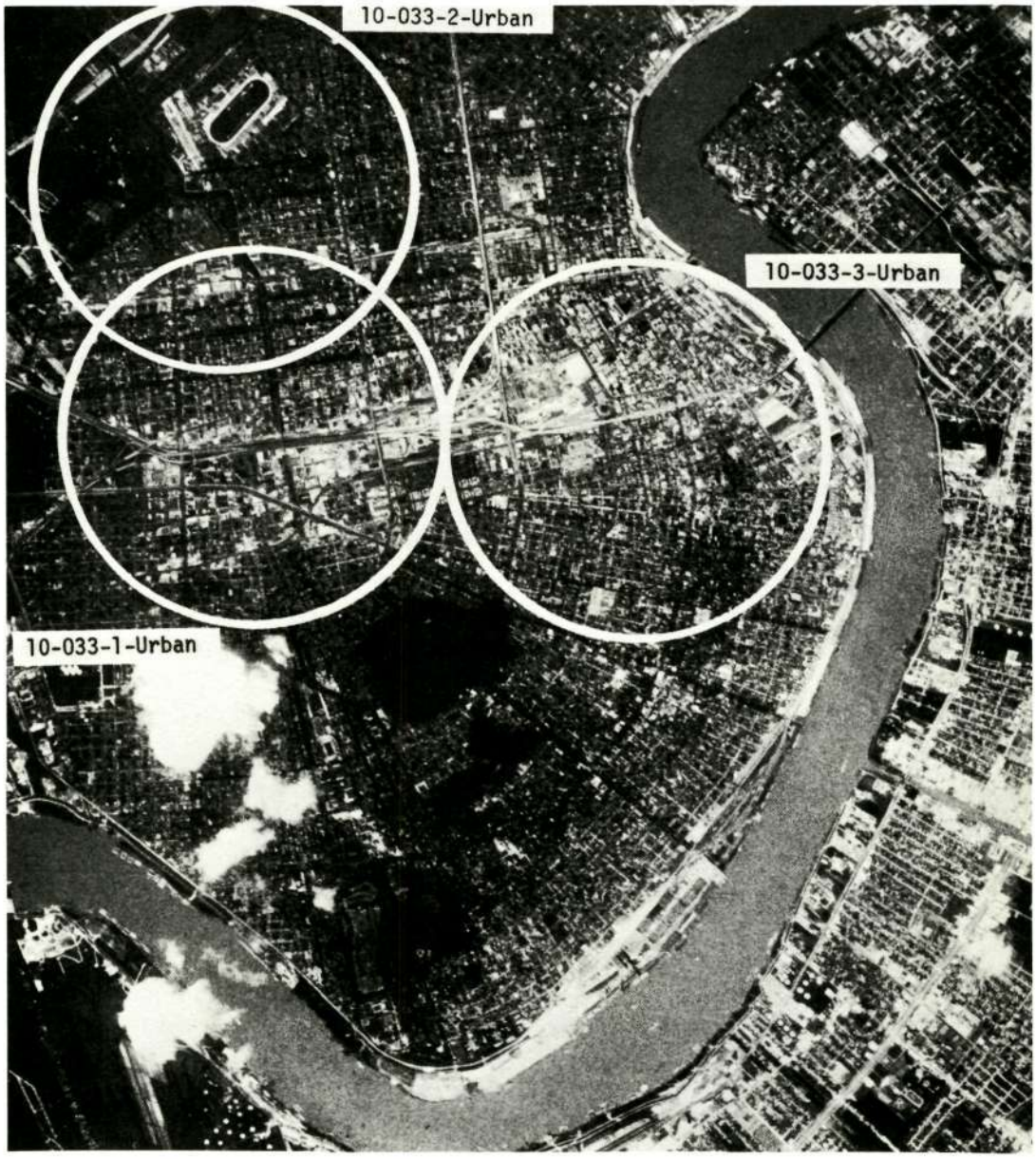

(a) Aircraft image, frame 10-033. Circled areas show scenes from which the diffraction patterns (b) were produced

Figure 3-1—New Orleans, Louisiana. Comparison between ERTS and aircraft images

10-033-1 Urban

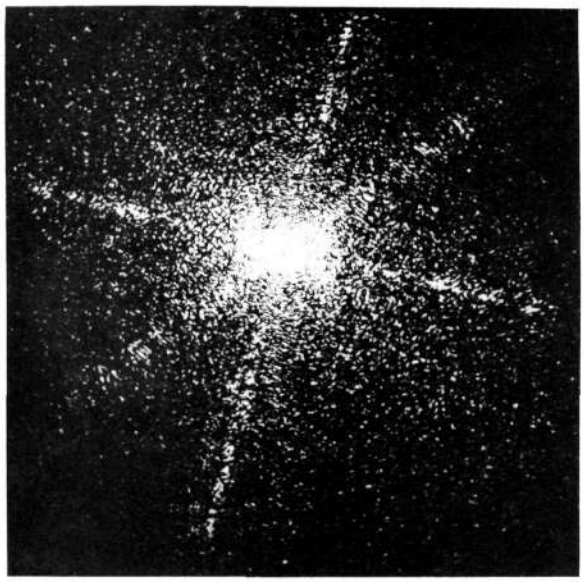

10-033-2 Urban

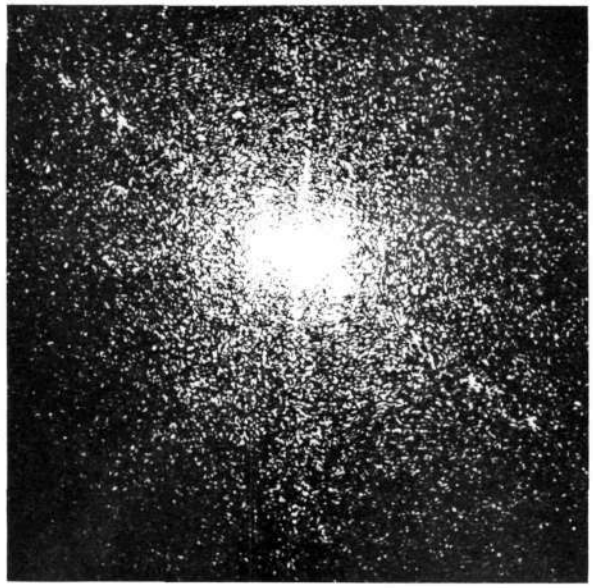

10-033-3 Urban

(b) Diffraction patterns from aircraft image, frame 10-033

Figure 3-1—New Orleans, Louisiana. Comparison between ERTS and aircraft images (Cont.)

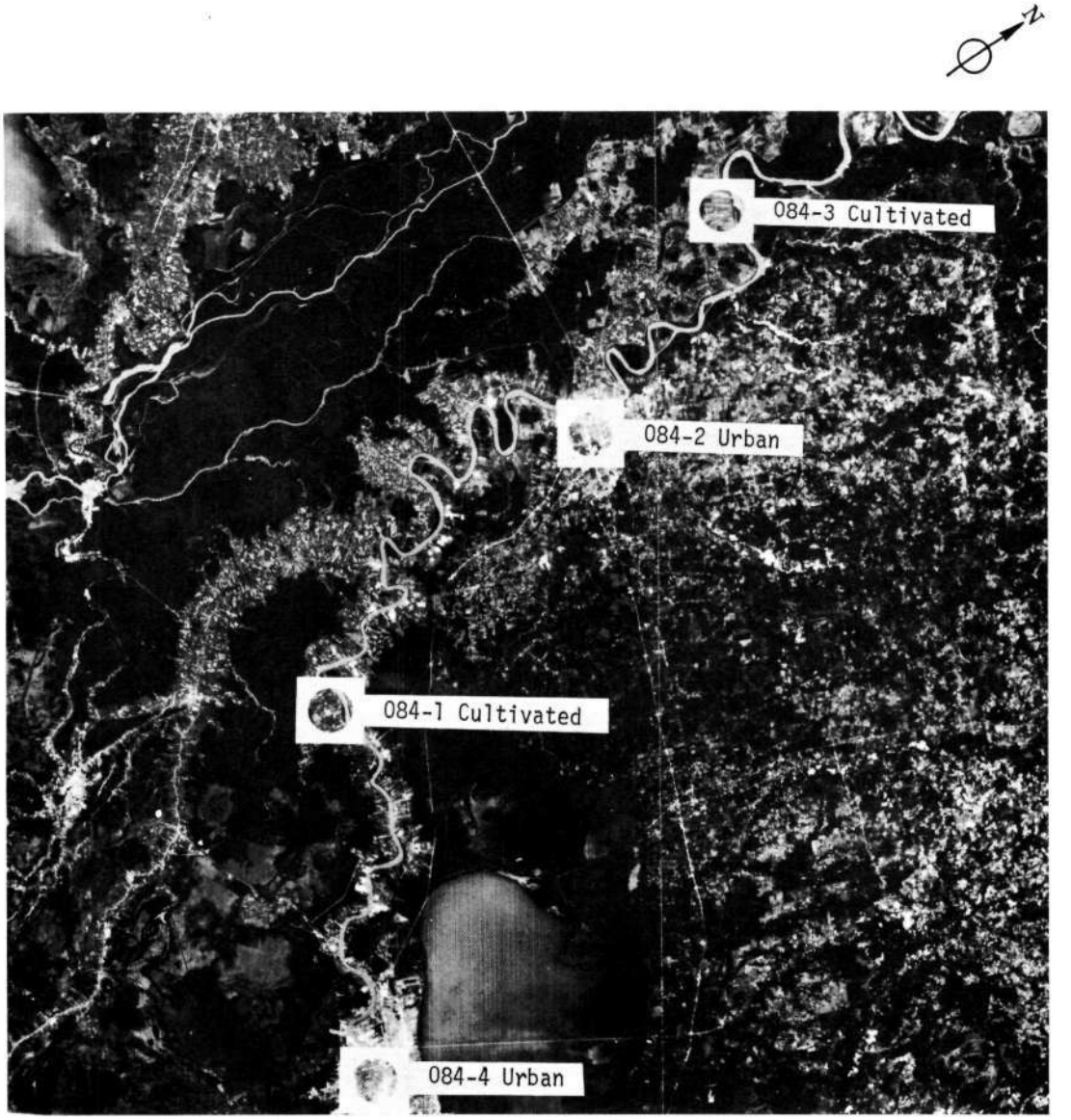

Figure 3-2(a)—New Orleans, Louisiana, ERTS-1 image No. 1070-16037-5. Circled areas show scenes from which diffraction patterns were produced

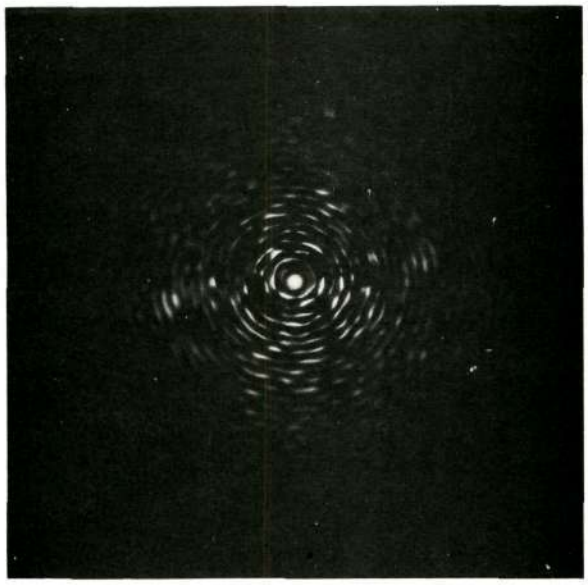

Diffraction pattern ERTS-084-4

New Orleans, La., ERTS-084-4

Figure 3-2(b) — New Orleans, Louisiana. Diffraction pattern and ERTS image from scene 084-4

New Orleans, La., ERTS-084-4

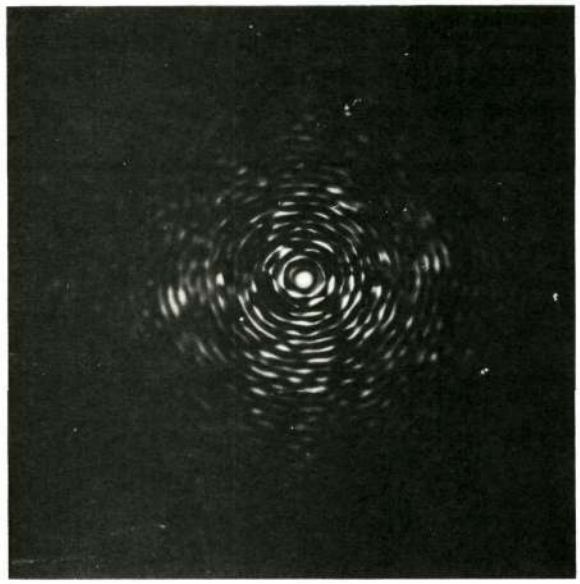

Diffraction pattern ERTS-084-4

Diffraction pattern from aircraft image

Figure 3-2(c) — New Orleans, Louisiana. Two diffraction patterns from same area: ERTS versus aircraft

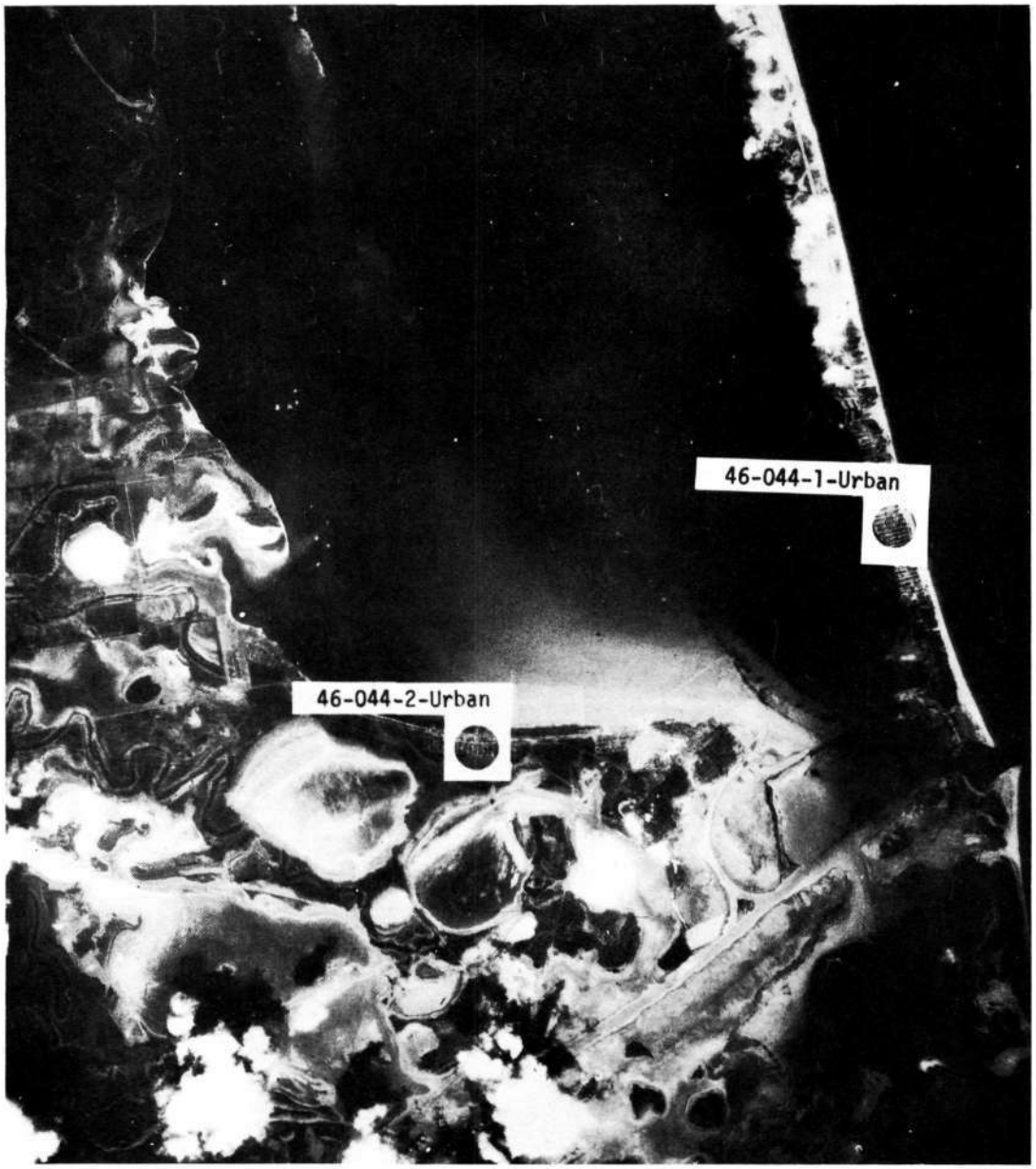

Figure 3-3 — Texas Gulf Coast. Aircraft image, frame 46-044. Circled areas show scenes from which diffraction patterns were produced.

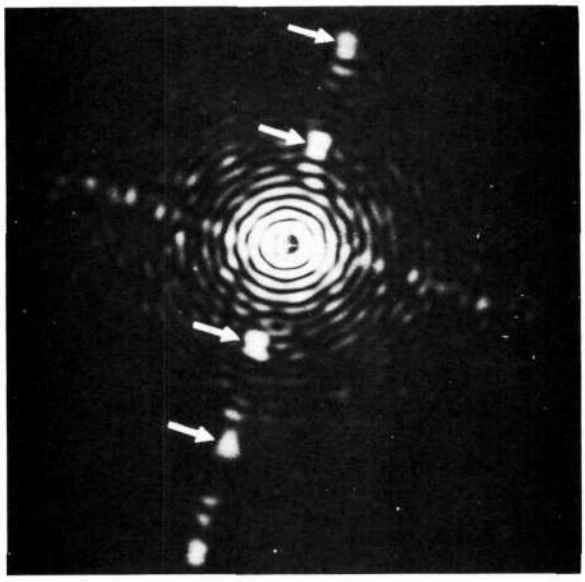

46-044-1 Urban

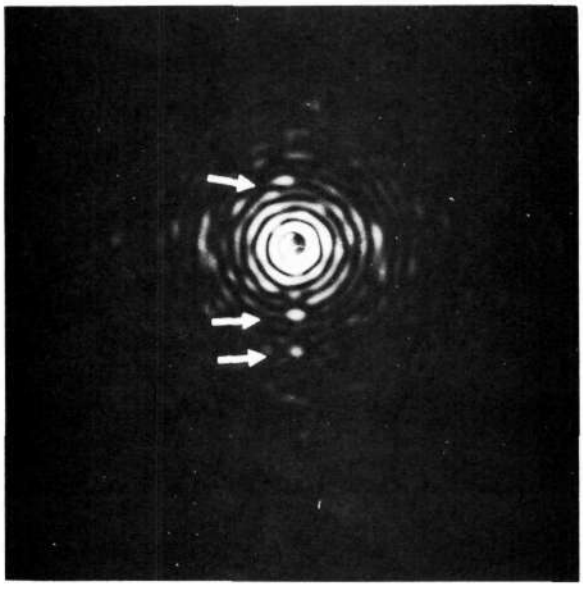

46-044-2 Urban

Figure 3-4—Texas Gulf Coast. Diffraction patterns from aircraft image, frame 46-044

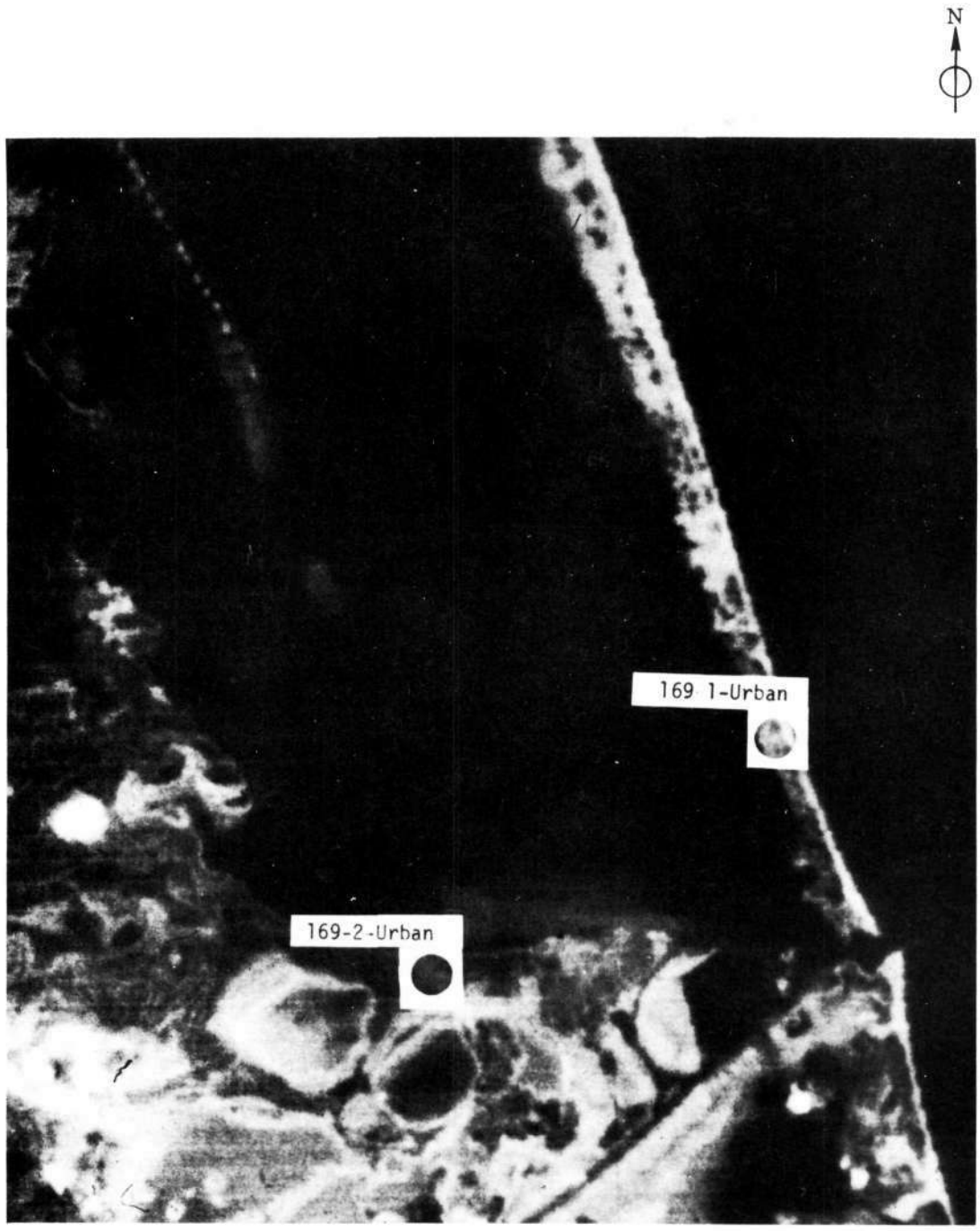

Figure 3-5—Texas Gulf Coast. Circled areas show scenes from which the diffraction patterns were produced. ERTS scene 169

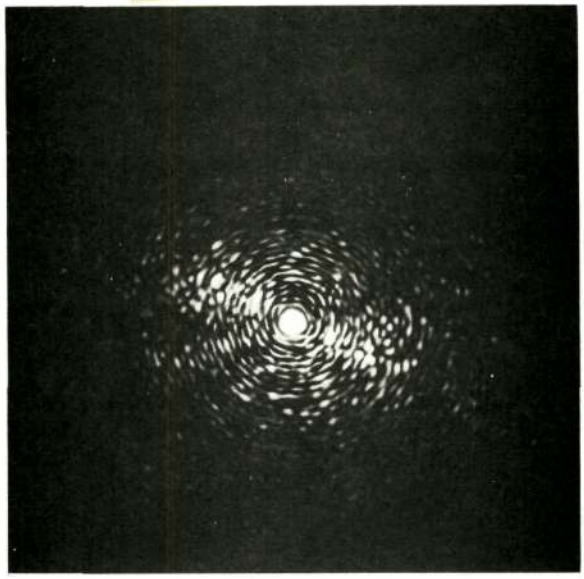

169-1 Urban

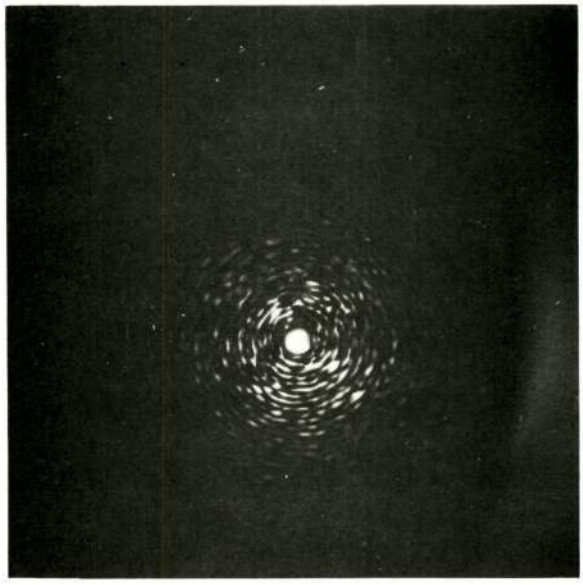

169-2 Urban

Figure 3-6—Texas Gulf Coast. Diffraction patterns from ERTS scene 169

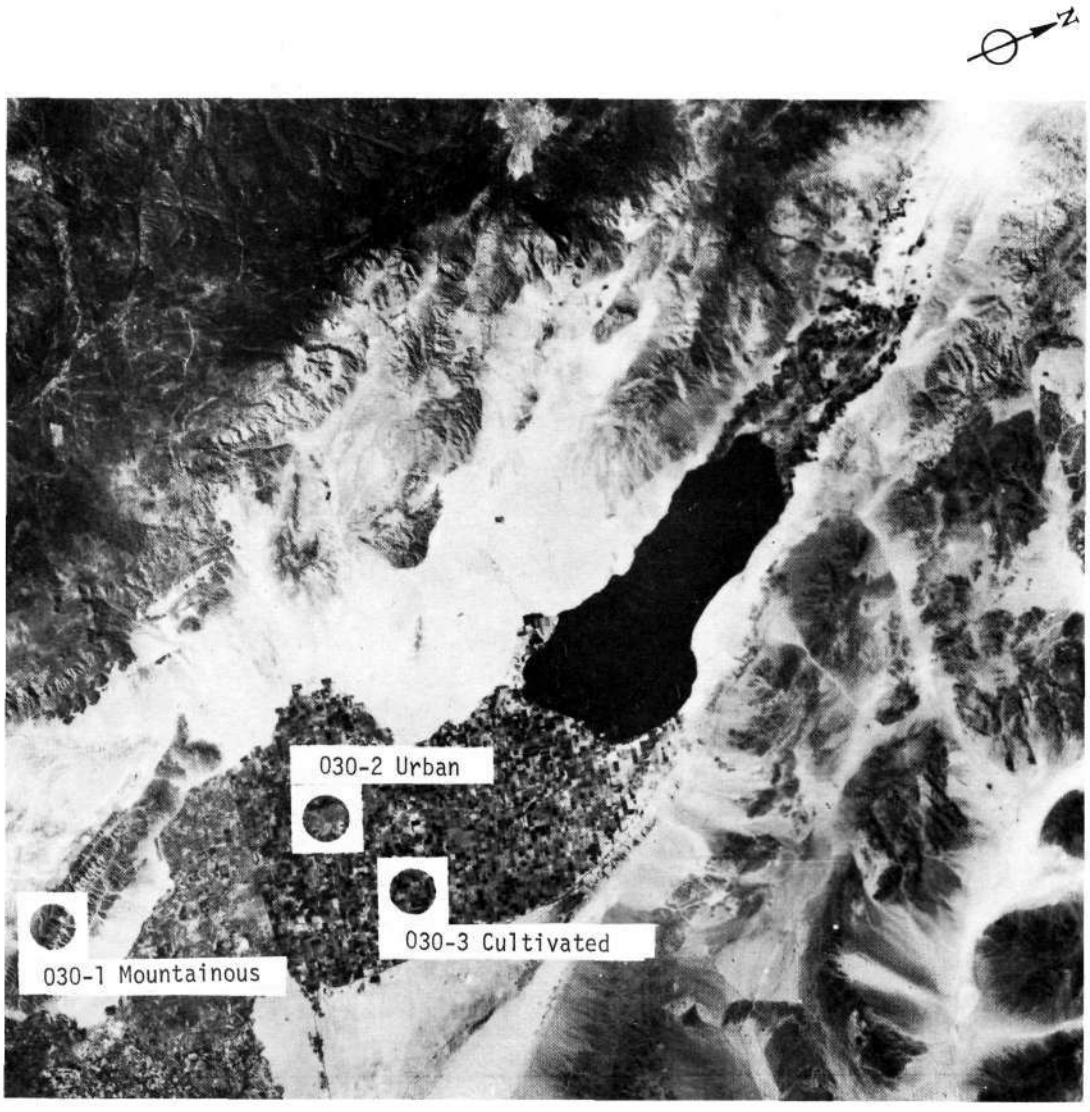

Figure 3-7—Salton Sea, California. Circled areas show scenes from which the diffraction patterns were produced

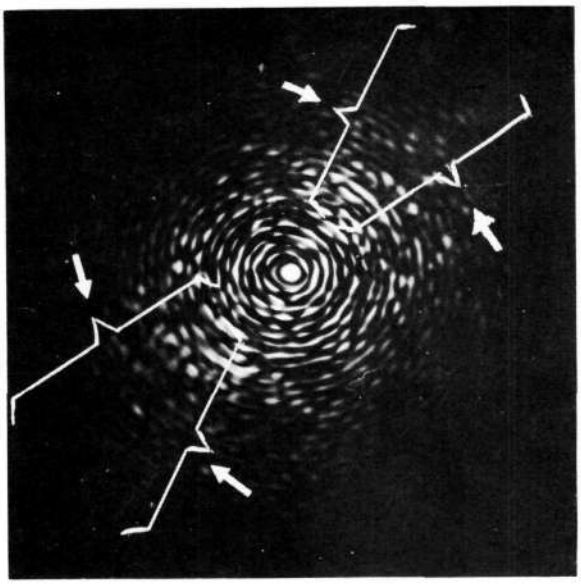

030-1 Mountainous

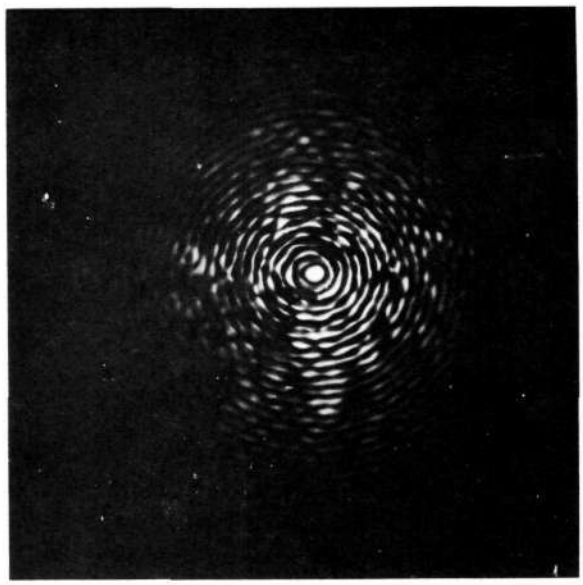

030-2 Urban

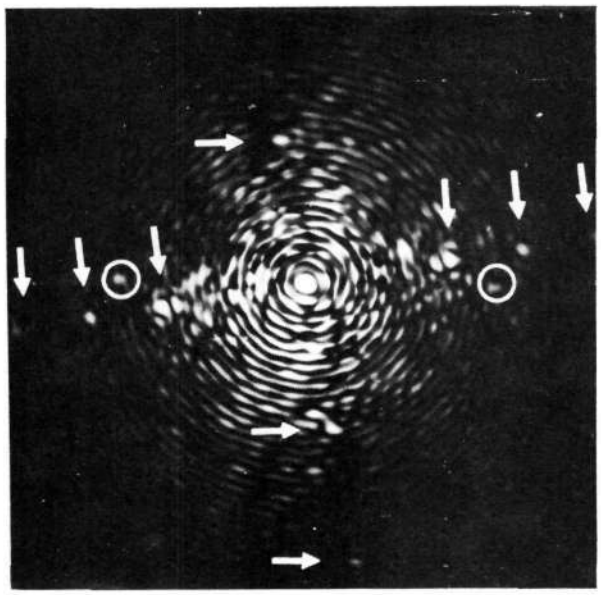

030-3 Cultivated

↑ Spots due to fields

◯ Spots due to scan lines

Figure 3-8—Salton Sea, California. Diffraction patterns from ERTS scene 030

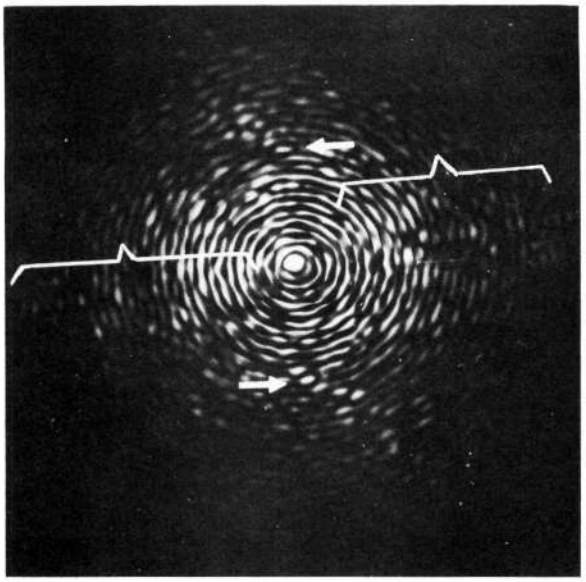

084-1 Cultivated

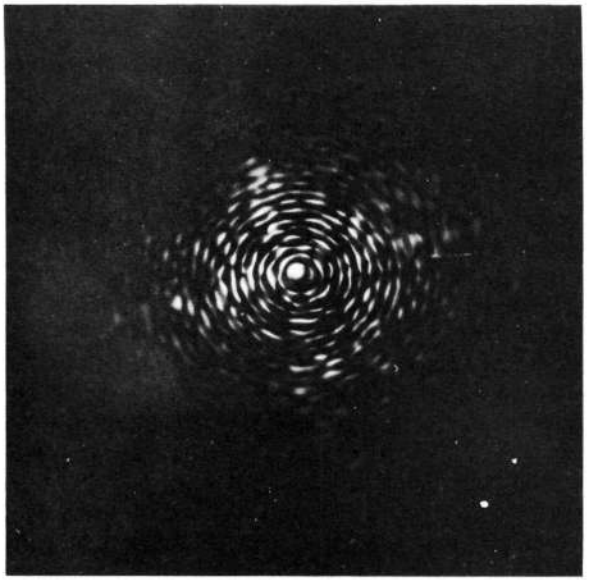

084-2 Urban

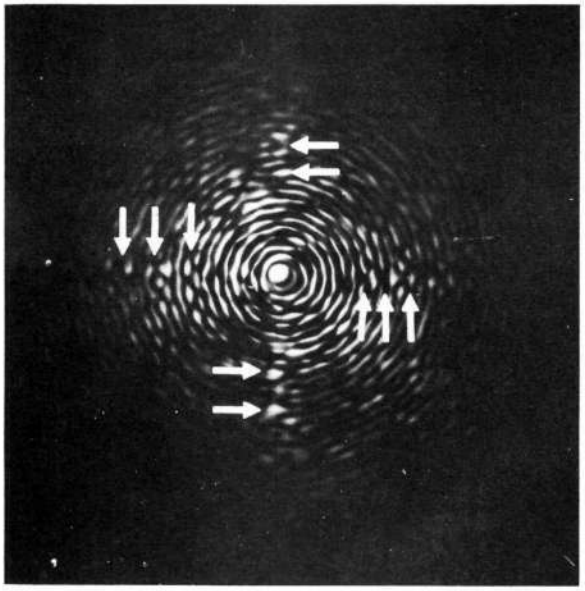

084-3 Cultivated

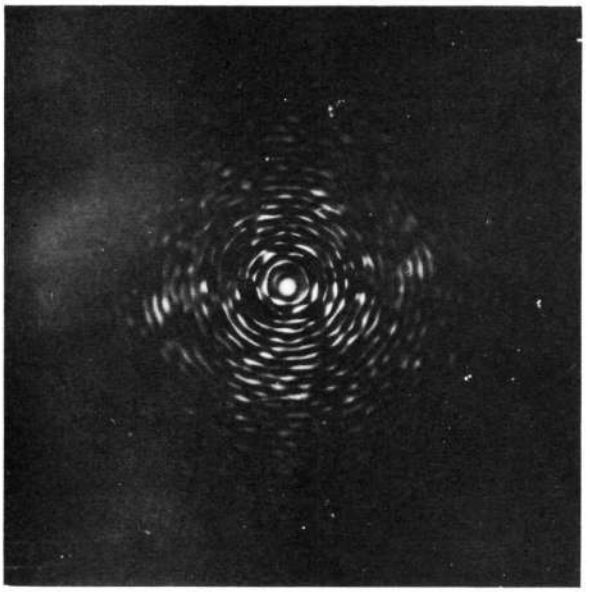

084-4 Urban

Figure 3-9—New Orleans, Louisiana. Diffraction patterns from ERTS scene 084

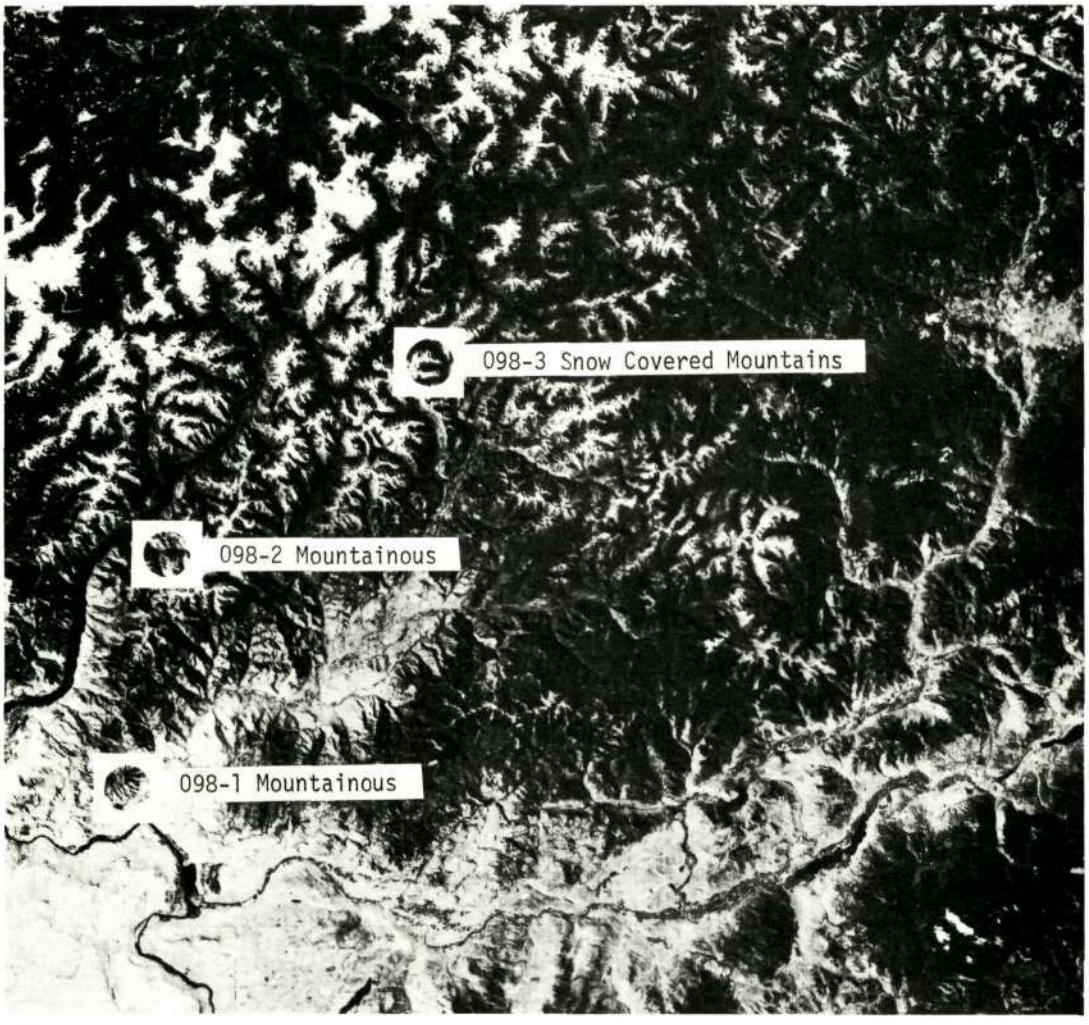

Figure 3-10—Cascade Mountains, Washington. Circled areas show scenes from which the diffraction patterns were produced

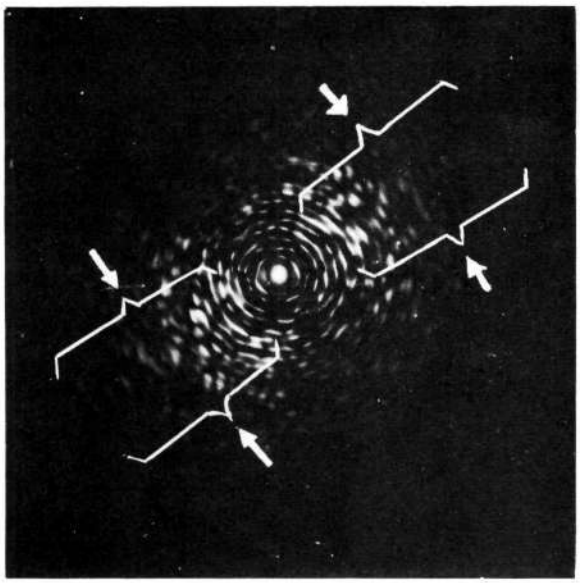

098-1 Mountainous

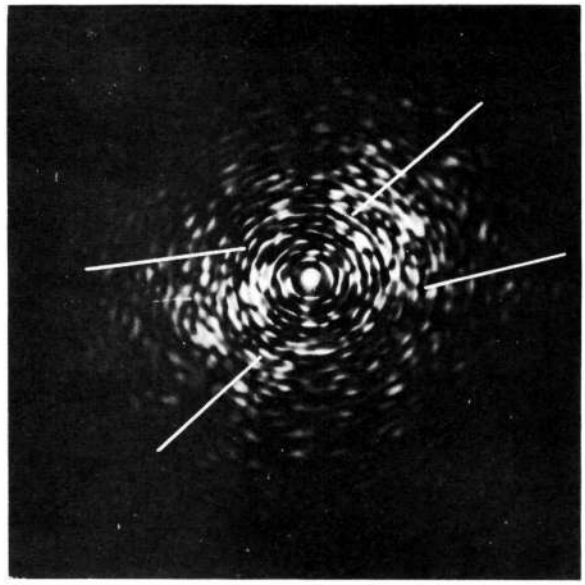

098-2 Mountainous

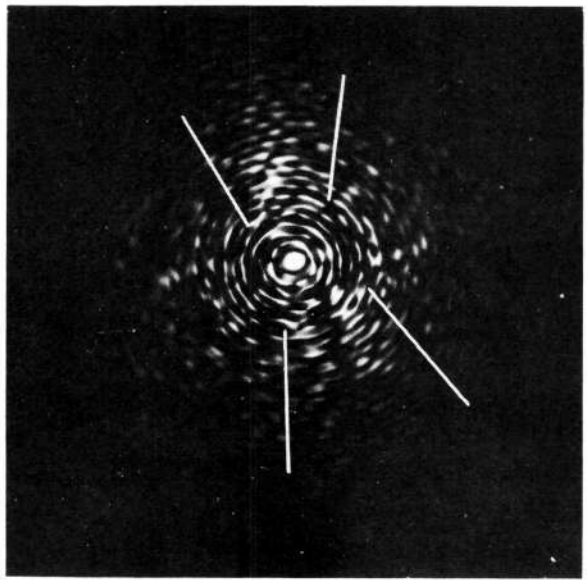

098-3 Snow-covered mountains

Figure 3-11—Cascade Mountains, Washington. Diffraction patterns from ERTS scene 098

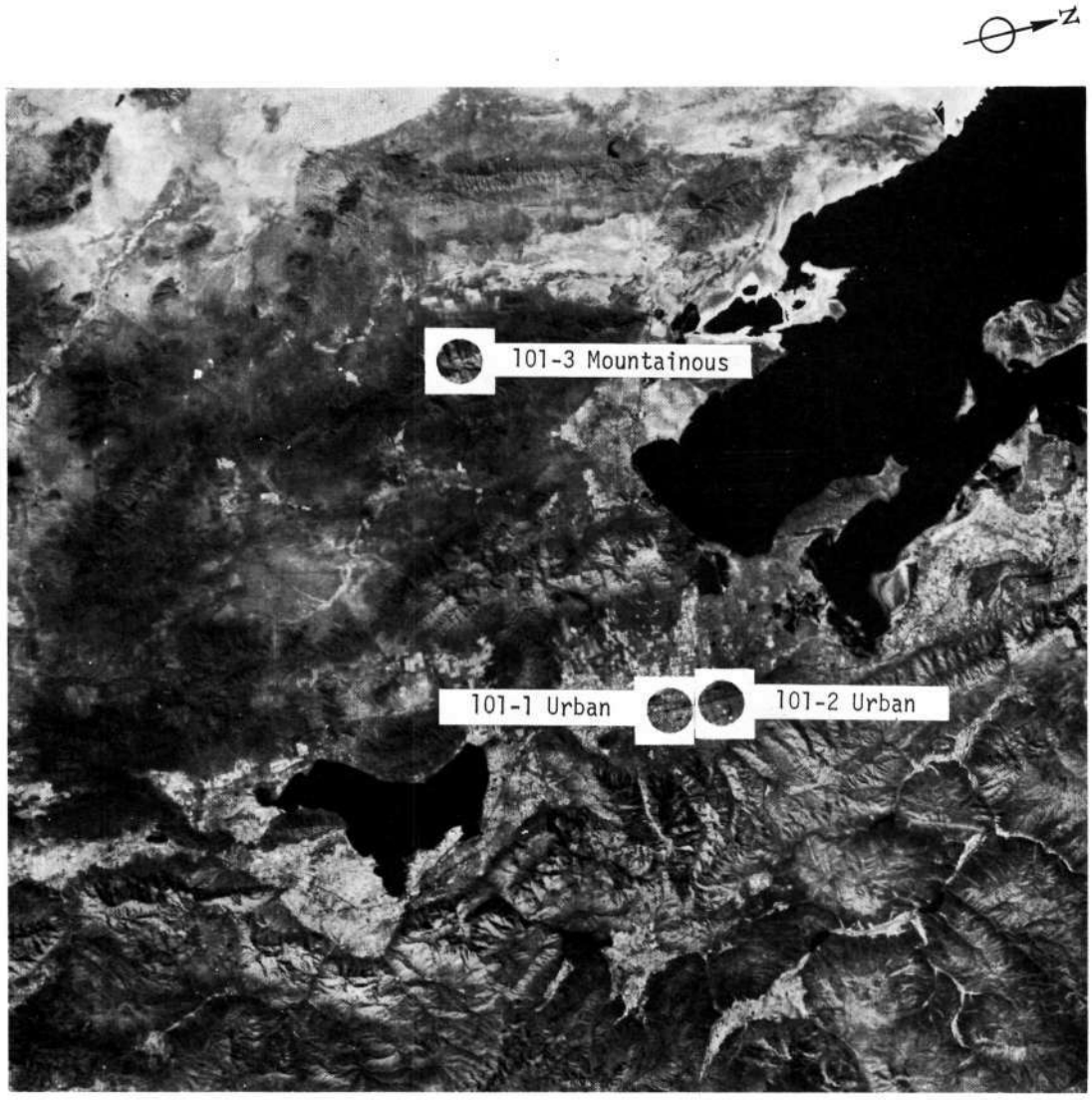

Figure 3-12—Great Salt Lake, Utah. Circled areas show scenes from which the diffraction patterns were produced

101-1 Urban

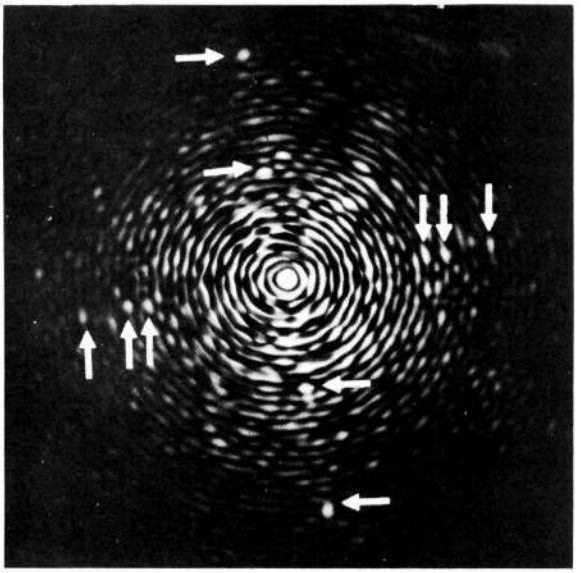

101-2 Urban

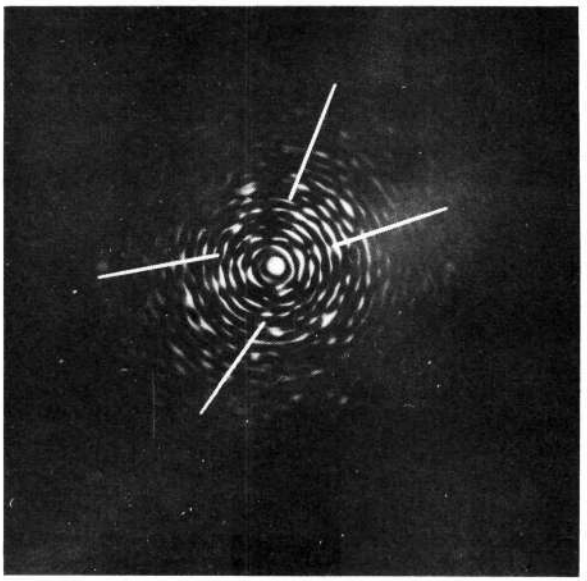

101-3 Mountainous

Figure 3-13 — Great Salt Lake, Utah. Diffraction patterns from ERTS scene 101

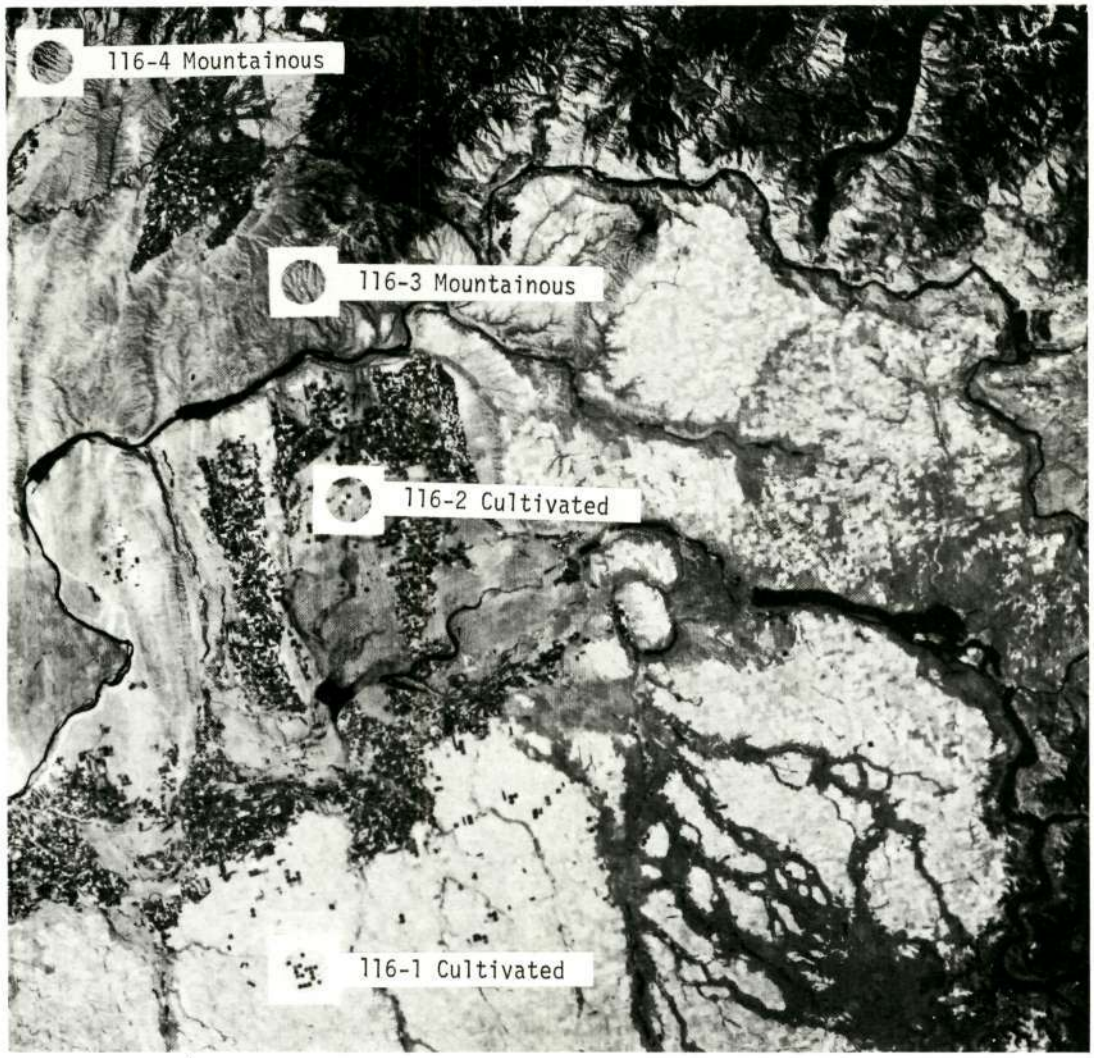

Figure 3-14—Cascade Mountains, Washington. Circled areas show scenes from which the diffraction patterns were produced

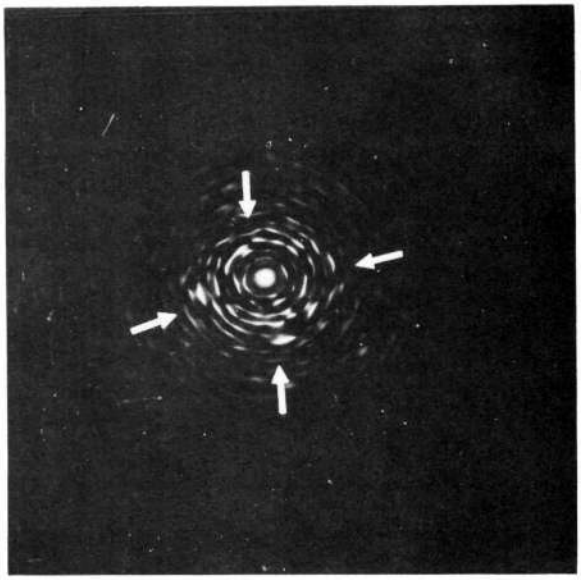

116-1 Cultivated

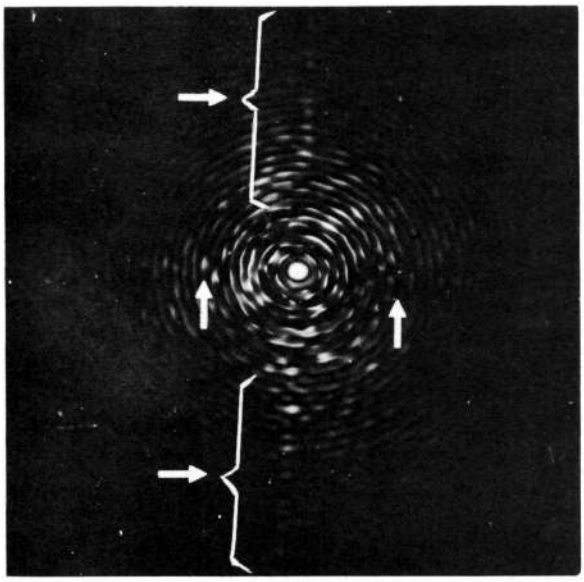

116-2 Cultivated

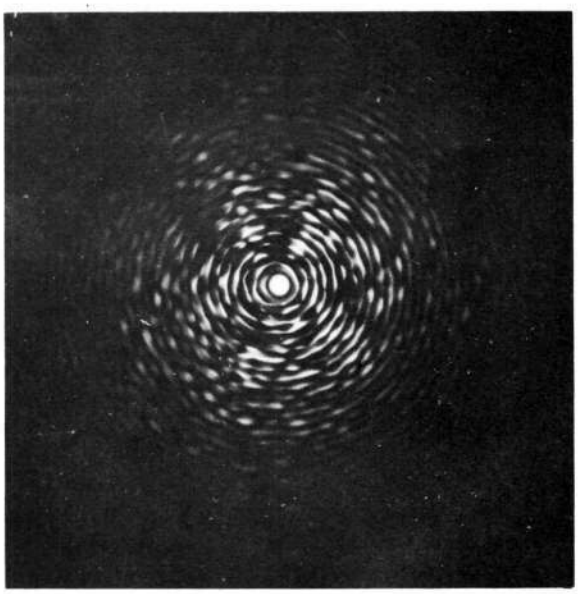

116-3 Mountainous

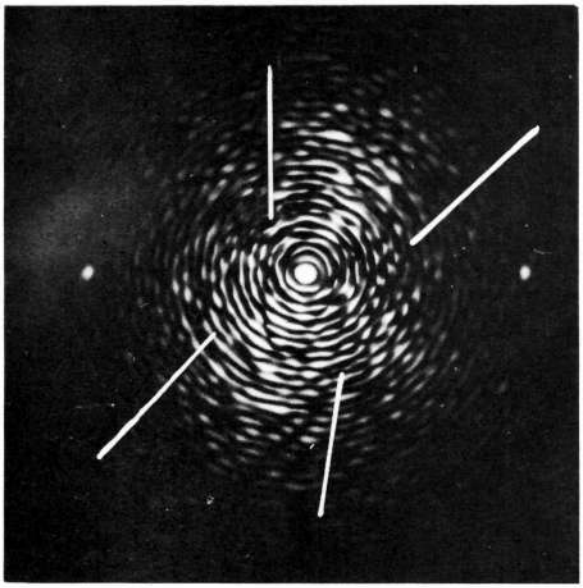

116-4 Mountainous

Figure 3-15—Cascade Mountains, Washington. Diffraction patterns from ERTS scene 116

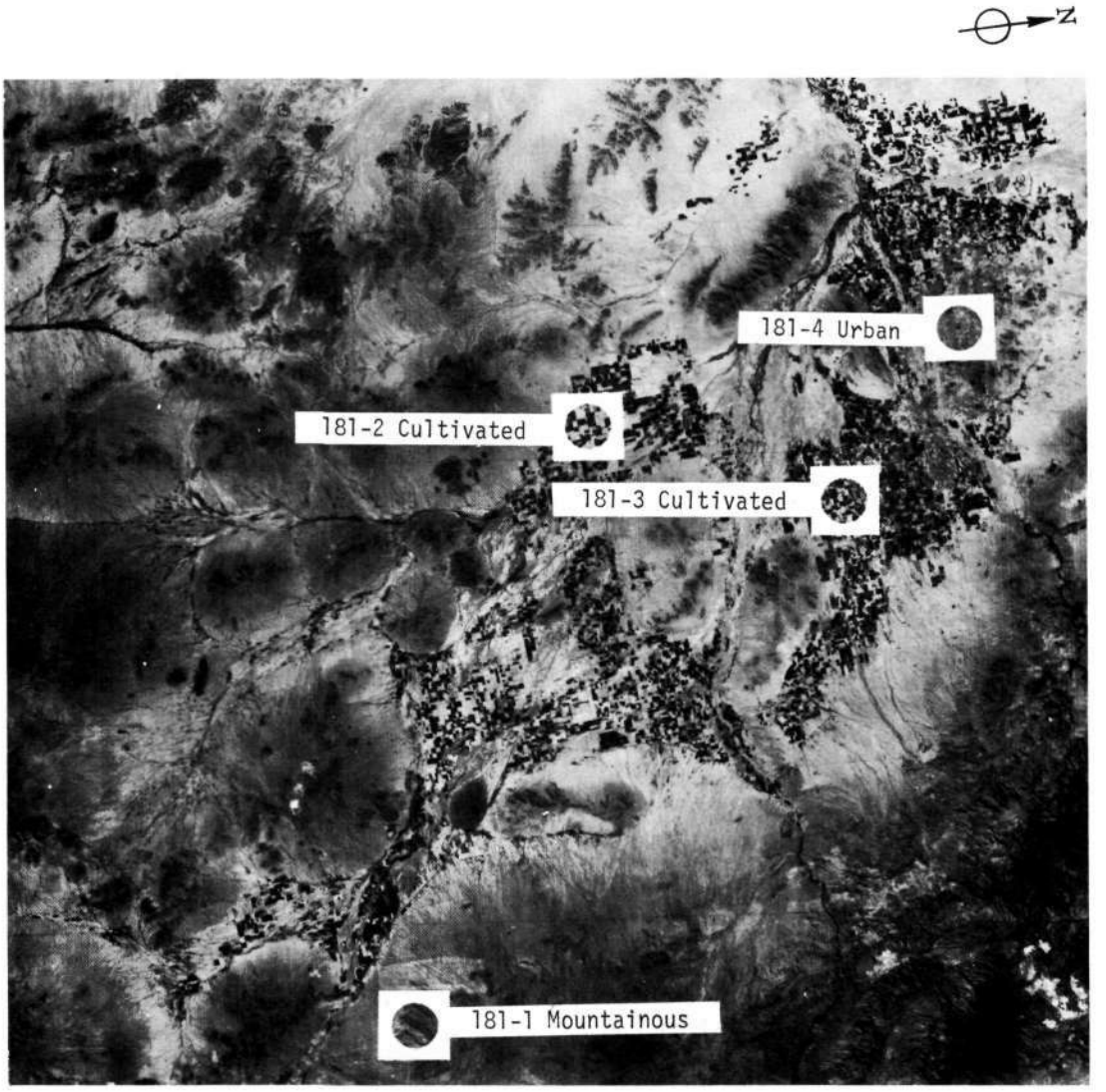

Figure 3-16— Phoenix, Arizona. Circled areas show scenes from which the diffraction patterns were produced

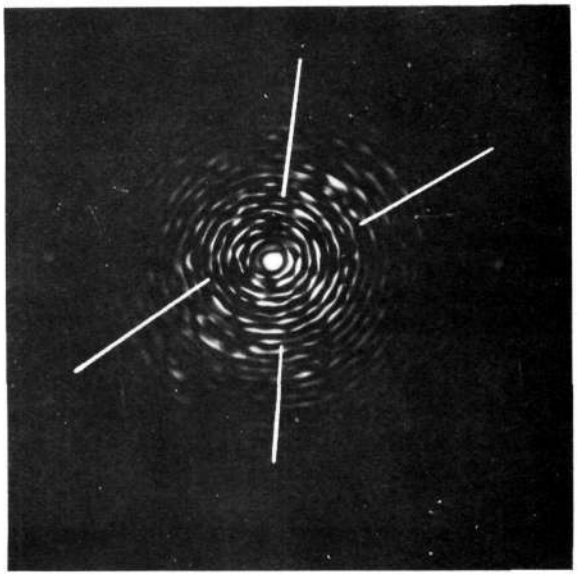

181-1 Mountainous

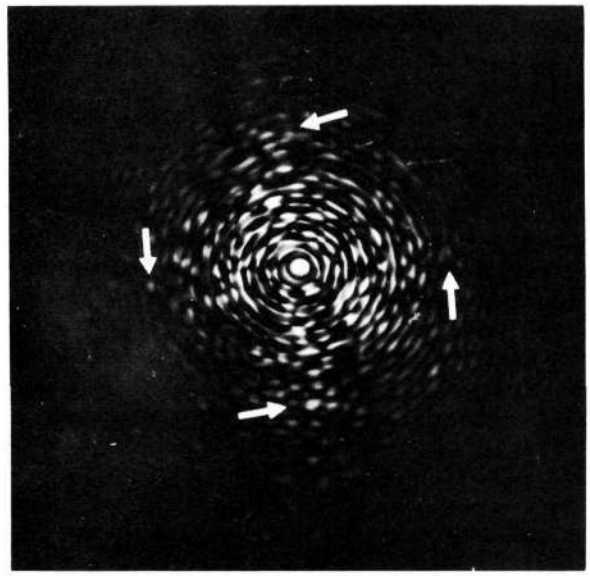

181-2 Cultivated

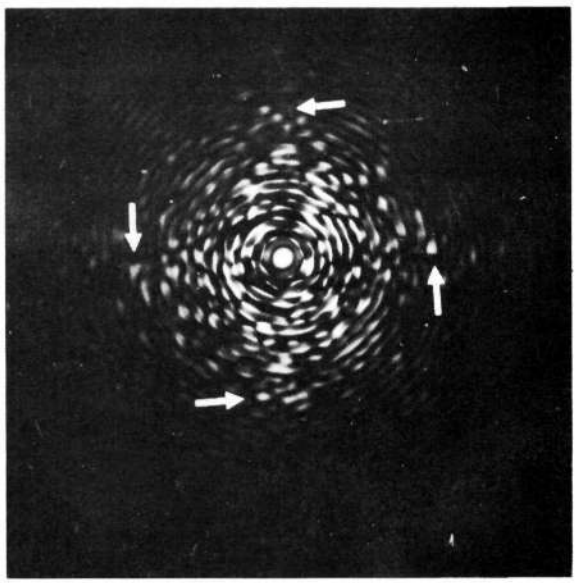

181-3 Cultivated

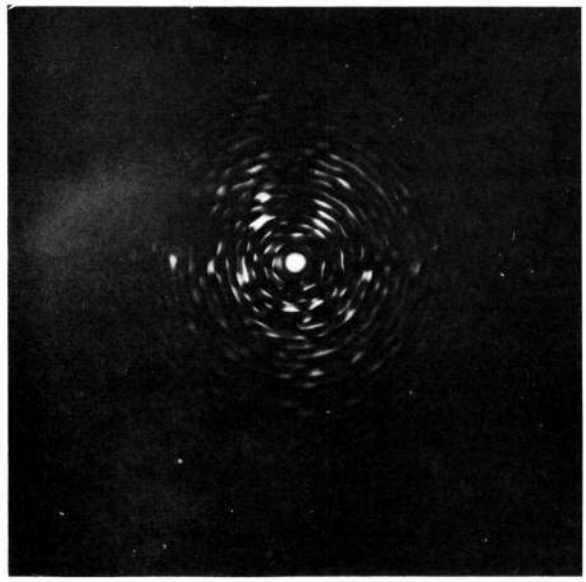

181-4 Urban

Figure 3-17— Phoenix, Arizona. Diffraction patterns from ERTS scene 181

Figure 3-18 — Phoenix, Arizona. Circled areas show scenes from which the diffraction patterns were produced

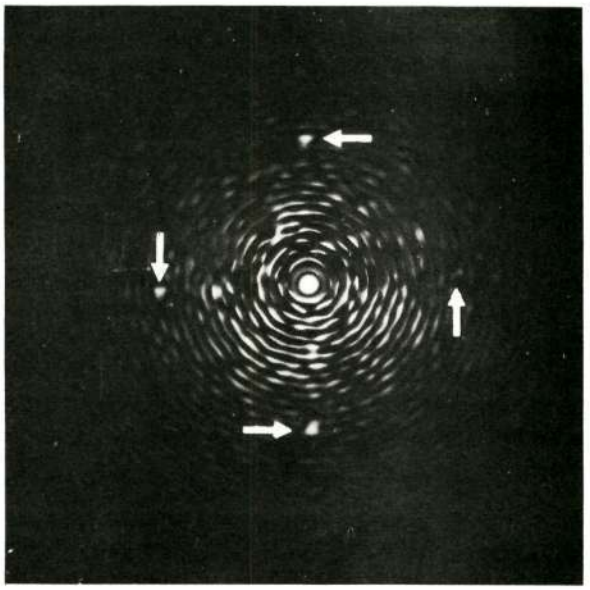

217-1 Urban

Figure 3-19 — Phoenix, Arizona. Diffraction pattern from ERTS scene 217

4. CONCLUSIONS

The search for terrain signatures has produced the following results:

- The diffraction patterns of mountains show clusters of intensity at low spatial frequencies and diffracted light spreading in wedge-shaped patterns (fans) away from the center. A unique signature for mountains may become evident when quantitative measurements are made on the diffraction patterns.
- For cultivated land, a signature consisting of orthogonal rows of frequency spots has been identified. For some images, the signature may be weak in relation to other components of the diffraction pattern.
- For urban areas, a signature consisting of orthogonal rows of frequency spots has been identified. This signature becomes evident only in the IR-2 image and cannot be confused with the signature for cultivated land, which is detected in the red band (0.6 to 0.7 micrometer). In the red band, a signature for some urban areas can be obtained with a high degree of probability from intersecting major highways.
- Broken clouds are recognized by an algorithm that operates on the image directly and, therefore, it is not necessary to develop a signature from diffraction patterns.
- A signature for hills has not been pursued because such a signature is expected to be similar to the mountain signature.
- Bodies of water have diffraction patterns with very low energy at frequencies other than the central lobe. Water can be identified by low reflectances in nearly all spectral bands and, therefore, the use of a spatial signature is usually redundant.
- Deserts also have diffraction patterns with low energy levels of light diffracted at most frequencies other than the central lobe and very low frequencies. A signature could possibly be developed for deserts but it is expected to be redundant if the multispectral information is utilized.
- Rivers and transportation networks are linear features that can be recognized by using algorithms operating directly on the image and testing for topographic characteristics. Although linear features have Fourier transforms that display high spatial frequency content in a direction perpendicular to the length of the feature (i.e., normal to the river banks), there is no indication that the Fourier transform provides better signature discrimination than the image itself.

In summation, the terrain features have been divided into three categories:

1. Features for which spatial signatures are not appropriate—deserts and bodies of water
2. Features that can best be identified by spatial signatures developed directly from an image—broken clouds, rivers, and transportation networks

3. Features that can be identified by spatial signatures isolated in the diffraction patterns or the Fourier transforms—cultivated land, some urban areas, mountains, and hills. The signature for mountains needs to be developed by quantitative measurements in the diffraction patterns.

5. FUTURE SPATIAL SIGNATURE WORK

Further diffraction pattern analysis is warranted only for mountainous terrain. Photometric measurements of diffraction patterns from mountainous terrain will be made. The patterns will be divided into a number of sectors by optical masks and the energy falling in each sector will be measured with a photometer. Then, the measurements will be normalized to the energy of the central lobe. The resulting data will be digitized and processed in the computer by the same clustering techniques employed for developing classes from multispectral data. If the measurements (treated as vectors) occupy a small volume of the measurement space, there is a high probability that the measurements contain a signature for mountains.

An alternative approach will be to develop (digitally) a gradient vector image directly from the mountain image and to utilize the distribution of orientation of the gradient vectors as a potential signature.

6. SIGNIFICANT RESULTS

Significant results of the diffraction pattern analysis of ERTS-1 imagery are the following:

- Signatures for cultivated land have been positively identified. This consists of orthogonal rows of frequency spots in the diffraction patterns
- Trends in signatures for mountainous terrain have been established. A unique signature for mountains may become evident when quantitative measurements are made on the diffraction patterns
- A signature similar to that found for cultivated areas has been found for urban areas. It is evident in a different spectral band and cannot be confused with the signature due to cultivated areas. This particular signature does not occur in all urban areas but signatures for these other urban areas have also been developed. These are due primarily to intersecting major highways
- Other terrain categories are identified by signatures developed directly from an image without recourse to Fourier transforms
- A Fourier plane filter has been developed. It has produced improved diffraction patterns and has greatly facilitated the terrain classification.

7. BIBLIOGRAPHY

1. Goodman, Joseph W., Introduction to Fourier Optics, McGraw-Hill Book Co., Inc., New York (1968), p. 86.
2. Born and Wolf, Principles of Optics, MacMillan Publishing Co., Inc., New York (1959), Chap. 8.
3. Smith, W., Modern Optical Engineering, McGraw-Hill Book Co., Inc., New York (1966).
4. Corbett, F., Diffraction Pattern Analysis for Image Quality Assessment, EIA conference, Washington, D. C. (Jan 8, 1973).
5. Palgen, J., Applicability of Pattern Recognition Techniques to the Analysis of Urban Quality from Satellites, Pattern Recognition: Vol. 2, No. 4, 255 (Dec 1970).